X INACTIVATION

PCGF3/5–PRC1 initiates Polycomb recruitment in X chromosome inactivation

Mafalda Almeida,[1] Greta Pintacuda,[1] Osamu Masui,[2] Yoko Koseki,[2] Michal Gdula,[1] Andrea Cerase,[1]* David Brown,[3] Arne Mould,[4] Cassandravictoria Innocent,[5] Manabu Nakayama,[6] Lothar Schermelleh,[5] Tatyana B. Nesterova,[1] Haruhiko Koseki,[2] Neil Brockdorff[1]†

Recruitment of the Polycomb repressive complexes PRC1 and PRC2 by Xist RNA is an important paradigm for chromatin regulation by long noncoding RNAs. Here, we show that the noncanonical Polycomb group RING finger 3/5 (PCGF3/5)–PRC1 complex initiates recruitment of both PRC1 and PRC2 in response to Xist RNA expression. PCGF3/5–PRC1–mediated ubiquitylation of histone H2A signals recruitment of other noncanonical PRC1 complexes and of PRC2, the latter leading to deposition of histone H3 lysine 27 methylation chromosome-wide. *Pcgf3/5* gene knockout results in female-specific embryo lethality and abrogates Xist-mediated gene repression, highlighting a key role for Polycomb in Xist-dependent chromosome silencing. Our findings overturn existing models for Polycomb recruitment by Xist RNA and establish precedence for H2AK119u1 in initiating Polycomb domain formation in a physiological context.

Polycomb proteins play an important role in developmental gene regulation, functioning primarily by establishing stable repressive chromatin states. Accordingly, the two major Polycomb repressor complexes, PRC1 and PRC2, catalyze posttranslational modifications of core histone proteins, mono-ubiquitylation of histone H2A lysine 119 (H2AK119u1) and methylation of histone H3 lysine 27 (H3K27me3), respectively [reviewed in (*1*)]. In mammalian cells, the noncoding RNA Xist recruits PRC1 and PRC2 to the inactive X chromosome (Xi) (*2*–*4*). Previous studies have proposed that Polycomb recruitment is initiated by direct binding of PRC2 to Xist RNA (*5*), although some evidence is difficult to reconcile with this model (*6*, *7*).

Noncanonical PRC1 complexes are recruited to Xi via an alternative pathway (*8*–*10*), and recent studies have demonstrated that PRC2 complexes can bind to PRC1-mediated H2AK119u1 (*11*–*14*), indicating that PRC1 could have a role in initiating Polycomb recruitment to the Xi. To test this possibility, we developed a mouse embryonic stem cell (mESC) model in which Xist RNA could be induced in the absence of RING1A/B, the core catalytic subunit of PRC1 (supplementary text S1 and fig. S1, A and B). As shown in Fig. 1, A to C, deletion of RING1A/B largely abolished Xist-dependent PRC2 (EZH2) recruitment and H3K27me3 deposition. Formation of Xist RNA domains was unaltered (Fig. 1, C and D).

We confirmed these findings by depleting H2AK119u1 using MG132, a proteasome inhibitor (*15*), in 3E mESCs that carry an inducible Xist transgene (*16*). H2AK119u1 was extensively depleted 6 hours after MG132 treatment (fig. S1, C and D), as reported previously (*9*). Xist-dependent recruitment of PRC2 (EED and H3K27me3 domains) was abolished (fig. S1, E and F). Together, these findings indicate that H2AK119u1 deposition is required for Xist-dependent recruitment of PRC2.

It has been proposed that the A-repeat region of Xist RNA—and/or a 4-kb region immediately downstream in Xist exon 1, designated XN and encompassing the F, B, and C repeats—mediates PRC2 recruitment in X inactivation (*5*, *7*). In light of our findings, we analyzed the role of these regions in Xist-dependent H2AK119u1 deposition. Thus, we established cell lines with inducible Xist transgenes carrying deletions of either the A-repeat or the XN region (fig. S2A). Immunofluorescence in situ hybridization (FISH) analysis of Xist RNA together with either H2AK119u1 or H3K27me3 revealed that deletion of the A-repeat had no effect, whereas deletion of the XN region entirely abolished Xist-dependent deposition of H2AK119u1 and H3K27me3 (fig. S2, B to E). These findings implicate the XN region in recruitment of PRC1 complex(es) required to initiate H2AK119u1 deposition on Xi.

In vertebrates, the catalytic core of PRC1 comprises RING1A/B and one of six homologs of the Polycomb group RING finger (PCGF) protein. Specific characteristics of PCGF1-6 define distinct subunit assemblies, subdivided into canonical and noncanonical PRC1 complexes (fig. S3A)

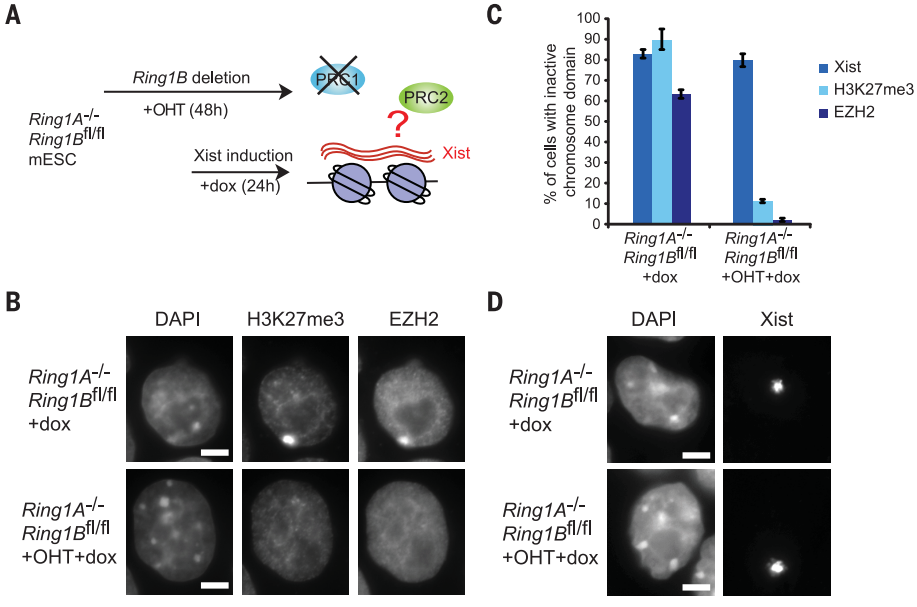

Fig. 1. H2AK119u1 mediates PRC2 recruitment by Xist RNA. (**A**) Schematic of the experiment. Tamoxifen, +OHT; doxycycline, +dox. (**B**) Examples of H3K27me3 and EZH2 immunofluorescence after 24 hours Xist induction. (**C**) Percentage of cells with domains for Xist, H3K27me3, and EZH2 in tamoxifen-treated and untreated cells after Xist induction for 24 hours. A minimum of 800 cells were counted in four biological repeats. Error bars indicate SD. (**D**) Xist RNA FISH illustrating deletion of *Ring1A/B* has no effect on Xist RNA domain formation.

[1]Developmental Epigenetics, Department of Biochemistry, University of Oxford, Oxford OX1 3QU, UK. [2]Laboratory for Developmental Genetics, RIKEN Center for Integrative Medical Sciences, 1-7-22 Suehiro, Tsurumi-ku, Yokohama 230-0045, Japan. [3]Chromatin Biology and Transcription, Department of Biochemistry, University of Oxford, Oxford OX1 3QU, UK. [4]Mammalian Development, Sir William Dunn School of Pathology, University of Oxford, South Parks Road, Oxford OX1 3RE, UK. [5]Micron Advanced BioImaging Unit, Department of Biochemistry, University of Oxford, Oxford OX1 3QU, UK. [6]Kazusa DNA Research Institute, 2-6-7 Kazusa-Kamatari, Kisarazu, Chiba, 292-0818, Japan.
*Present address: European Molecular Biology Laboratory Monterotondo, Adriano Buzzati–Traverso Campus, Via Ramarini 32, 00015 Monterotondo, Italy. †**Corresponding author.**
Email: neil.brockdorff@bioch.ox.ac.uk

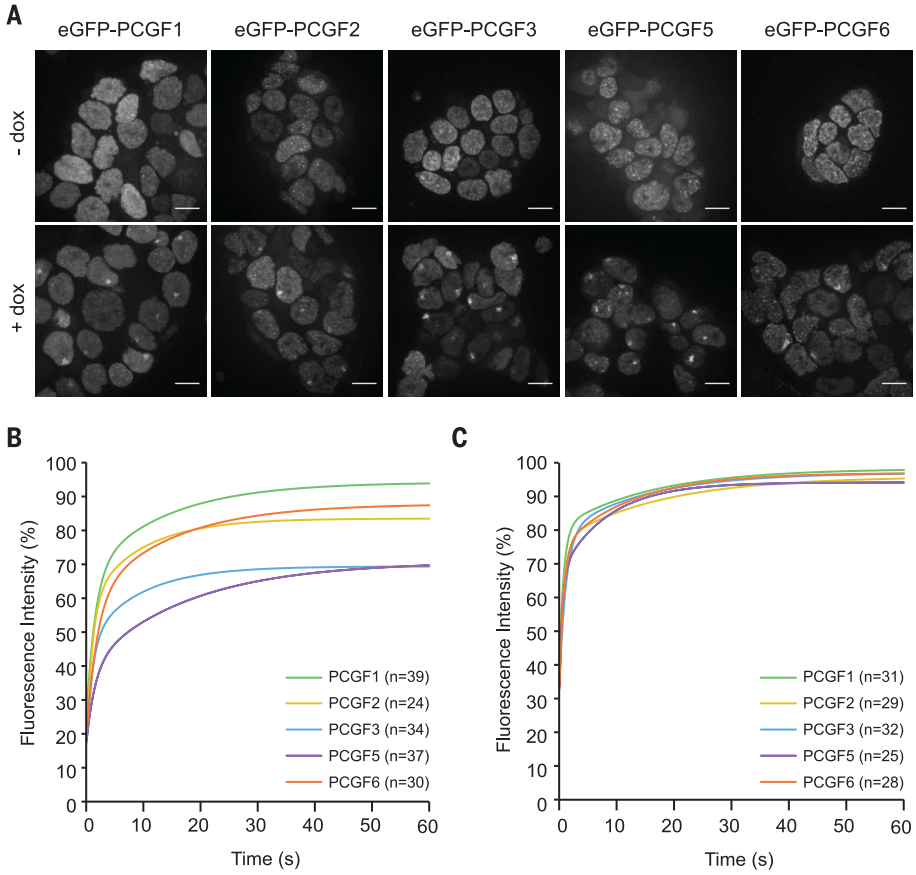

Fig. 2. Xist-dependent localization and dynamics of noncanonical PRC1 complexes. (**A**) Images illustrating focal enrichment of eGFP-PCGF fusion proteins after induction of Xist RNA for 24 hours in 3E-H mESCs sublines (+dox). Focal enrichment is not seen in uninduced cells (−dox). Images are maximum-intensity projections of six consecutive *z*-stacks. Scale bar, 10 μm. (**B**) FRAP of eGFP-PCGF fusion proteins within Xist RNA domains. (**C**) FRAP of eGFP-PCGF fusion proteins within randomly selected regions of the nucleoplasm. In (B) and (C), data from single cells was fitted with a biexponential equation. Curves represent average of the fit from a number (*n*) of cells.

(*9*, *17*). PCGF2 and PCGF4 are close homologs, as are PCGF3 and PCGF5 (fig. S3B). To determine which of the different PRC1 complexes are recruited to Xist RNA domains, we stably expressed N-terminal enhanced green fluorescent protein (eGFP) fusion proteins for PCGF1, PCGF2 (which, together with PCGF4, contributes to either canonical or noncanonical PRC1 complexes), PCGF3, PCGF5, and PCGF6 in 3E-H–inducible Xist mESCs (fig. S3C) (*18*). All of the eGFP-PCGF fusion proteins were assembled into PRC1 complexes, as judged with coimmunoprecipitation analysis of the RING1B subunit (fig. S3D). Live cell confocal imaging revealed Xist-dependent concentration of each eGFP-PCGF fusion protein within a single discrete subnuclear region, referred to henceforth as Xist RNA domains (Fig. 2A and movie S1). Localization of eGFP-PCGF fusion proteins to Xist RNA domains was also observed by using immunofluorescence (IF), albeit to varying degrees (fig. S3, E and F). The variable efficiency of detection with IF likely reflects the dynamic behavior of different PRC1 complexes (supplementary text S2).

The localization of eGFP-PCGF fusion proteins over Xist RNA domains enabled us to compare the dynamic behavior of different PRC1 complexes using fluorescence recovery after photobleaching (FRAP). Thus, for each eGFP-PCGF fusion protein we took FRAP measurements both within Xist RNA domains and also in a randomly selected nucleoplasmic region. For eGFP-PCGF1, eGFP-PCGF2, and eGFP-PCGF6, the average recovery within Xist RNA domains was in the order of a few seconds. In contrast, for eGFP-PCGF3 and eGFP-PCGF5, a significant immobile fraction, retained over the time-course of the experiment (60 s), indicated a relatively stable interaction (Fig. 2B and fig. S4, A, B, and D). We refer to these interaction modes as transient (<60 s) and stable (≥60 s), respectively. In the nucleoplasm, all of the eGFP-PCGF proteins showed similar transient dynamic behavior, fully recovering over a time scale of seconds (Fig. 2C and fig. S4, B to D). This suggests that the distinct behavior of eGFP-PCGF3 and eGFP-PCGF5 reflects differences in their interactions with the Xist RNA domain, rather than systematic differences between the eGFP-fusion proteins or the cell lines. These conclusions were further supported by analysis of the rate of turnover ($t_{1/2}$), determined by fitting recovery curves with a biexponential equation (supplementary text S3 and fig. S4C). The FRAP experiments thus reveal a qualitative difference between complexes formed by PCGF1/2/6, which interact transiently with the Xist RNA domain, and eGFP-PCGF3/5–PRC1, which additionally form stable interactions.

The noncanonical PRC1 subunit RYBP, and/or its homolog YAF2, can bind to H2AK119u1, mediated by a NZF domain (*9*, *17*, *19*, *20*). To test whether this interaction could contribute to localization of PRC1 complexes within Xist RNA domains, we generated *Rybp*$^{-/-}$*Yaf2*$^{-/-}$ mESCs (supplementary text S4 and fig. S5, A and B). Recruitment of PRC1 (and PRC2) by Xist RNA was retained, as indicated by accumulation of H2AK119u1 and H3K27me3 (fig. S5, C and E). However, quantification of domain size and time-course analysis revealed that deposition of H2AK119u1 and H3K27me3 is impaired relative to wild-type mESCs (supplementary text S5 and fig. S5, D and E). The time-course analysis (fig. S5E) further illustrates that H2AK119u1 deposition within Xist RNA domains precedes H3K27me3, supporting that PRC1 initiates PRC2 recruitment.

Although PRC1 activity over Xist RNA domains is evident in *Rybp*$^{-/-}$ *Yaf2*$^{-/-}$ mESCs, we were unable to detect enrichment of eGFP-PCGF fusion proteins using either live cell imaging or conventional IF (fig. S6A and movies S2 to S6), likely reflecting their reduced levels relative to background. Consistent with this idea, we were able to detect localization of eGFP-PCGF3 and eGFP-PCGF5 using a modified IF protocol (supplementary text S6 and fig S6B).

We went on to test whether reduced Xist RNA domain enrichment of eGFP-PCGF proteins in *Rybp*$^{-/-}$*Yaf2*$^{-/-}$ mESCs is linked to the ability of RYBP to bind H2AK119u1. Thus, we complemented *Rybp*$^{-/-}$*Yaf2*$^{-/-}$ mESCs using constructs that express mCherry-tagged wild-type RYBP or a mutant protein, RYBP TF-AA, which has three point mutations in the NZF domain that abrogates the interaction with H2AK119u1 (*20*). As illustrated in Fig. 3, wild-type, but not TF-AA, RYBP restored Xist RNA domain enrichment of eGFP-PCGF fusion proteins. We conclude that RYBP/YAF2 binding to H2AK119u1 likely underpins the transient interaction of noncanonical PRC1 complexes with Xist RNA domains but does not account for stable interaction of PCGF3/5–PRC1 complexes.

We next tested the role of PCGF3/5–PRC1 complexes in initiating Polycomb recruitment by Xist RNA. Thus, we engineered a series of ESC lines with doxycycline-inducible Xist transgenes in which we could investigate the importance of PCGF3 and PCGF5 either alone or together (fig. S7, A, B, D, and E). A conditional knockout mESC line for *Pcgf1* was used as a negative control (supplementary text S7 and fig. S7, A to C). We then tested whether H2AK119u1 and H3K27me3 deposition occur over Xist RNA domains 24 hours after induction of the Xist transgene (Fig. 4A).

Deletion of either *Pcgf1* or *Pcgf5* alone had no effect on Xist-dependent H2AK119u1 and H3K27me3 deposition (fig. S8, A to D). Deletion of *Pcgf3* alone resulted in a small but significant decrease of both H2AK119u1- and H3K27me3-positive domains (fig. S8, C and D). Strikingly, deletion of both *Pcgf3* and *Pcgf5* together strongly reduced Xist-dependent H2AK119u1 and H3K27me3 deposition (Fig. 4, B and C, and fig. S8, C, D, and E). Moreover, in *Pcgf3*$^{-/-}$*Pcgf5*$^{-/-}$ mESCs that were cultured with tamoxifen for 96 hours and then expanded before inducing Xist expression, H2AK119u1 and/or H3K27me3 domains were entirely abolished (Fig. 4C). Global levels of H2AK119u1, H3K27me3, and PRC1 subunits were unaffected (fig. S8F), indicating that the observed deficiency is specific to Polycomb recruitment by Xist RNA.

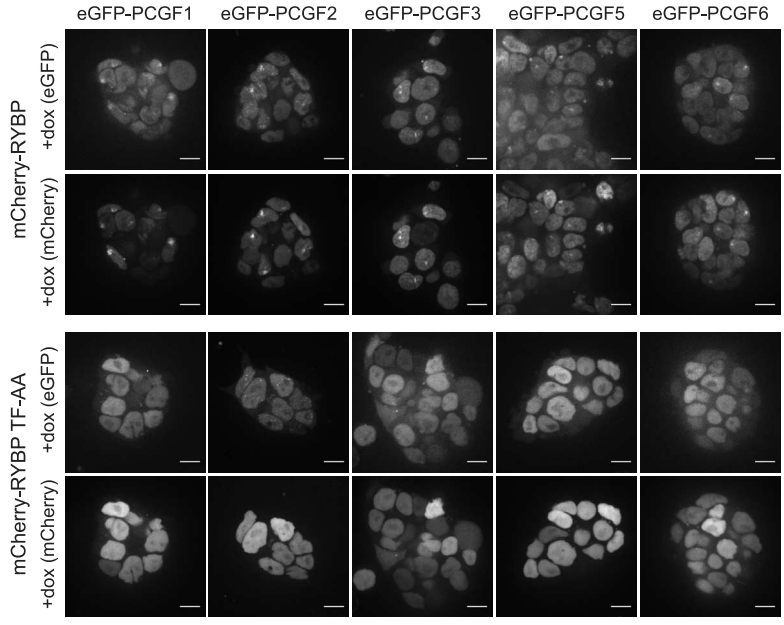

Fig. 3. RYBP/YAF2 interaction with H2AK119u1 contributes to Xist-dependent enrichment of noncanonical PRC1 complexes. Images illustrating distribution of eGFP-PCGF proteins in *Rybp*$^{-/-}$*Yaf2*$^{-/-}$ mESC lines complemented with wild-type mCherry-RYBP, or mCherry-RYBP TF-AA mutant after Xist induction (+dox) for 24 hours. Images are maximum-intensity projections of six consecutive *z*-stacks. Scale bar, 10 μm.

Our results suggest that PCGF3/5–PRC1–mediated H2AK119u1 initiates Xist-dependent recruitment both of other noncanonical PRC1 complexes and of PRC2. In support of this model, Xist-dependent recruitment of eGFP-PCGF3 or eGFP-PCGF5 occurs in the absence of PRC2 and H3K27me3 (supplementary text S8 and fig. S9A) and is abolished in cells expressing the ΔXN Xist RNA (supplementary text S9 and fig. S9, B and C). Moreover, analysis by three-dimensional structured illumination (3D-SIM) super-resolution microscopy revealed that PCGF3/5–PRC1 is significantly closer to Xist RNA than are other noncanonical PRC1 complexes (supplementary text S10 and fig. S10, A and B).

To verify our results in the context of X inactivation in vivo, we went on to establish *Pcgf3* and *Pcgf5* conditional knockout mouse lines (figs. S7D and S11A). Analysis of embryonic day 7.5 (E7.5) XX *Pcgf3*$^{-/-}$*Pcgf5*$^{-/-}$ embryos revealed complete absence of H2AK119u1 and H3K27me3 on Xi in embryonic and extraembryonic regions (Fig. 4D, fig. S11, B to E, and supplementary text S11). We further analyzed progeny from *Pcgf3*$^{+/-}$:*Pcgf5*$^{+/-}$ heterozygote crosses. *Pcgf3*$^{-/-}$*Pcgf5*$^{-/-}$ were not recovered among live-born progeny. At mid-gestation stages (E9.5 and E10.5), we recovered male *Pcgf3*$^{-/-}$*Pcgf5*$^{-/-}$ conceptuses in

Fig. 4. PCGF3/5–PRC1 initiates Polycomb recruitment to facilitate chromosome silencing by Xist RNA. (**A**) Schematic representation of PCGF knockout experiments. Tamoxifen, +OHT; doxycycline, +dox. (**B**) Images illustrating accumulation of H2AK119u1 over Xist RNA domains in the presence and absence of PCGF proteins. (**C**) Scoring data representing a minimum of 300 cells in three replicates is summarized in the bar chart. Error bars show SD. Significant differences (Student's *t* test) are indicated (**$P < 0.001$). (**D**) Immunofluorescence analysis of H2AK119u1 and H3K27me3 domains in *Pcgf3*$^{-/-}$:*Pcgf5*$^{-/-}$ and *Pcgf3*$^{fl/fl}$:*Pcgf5*$^{fl/fl}$ female embryos at E7.5. Images show representative single focal plane scans through epiblast. Scale bar, 20 μm. (**E**) Genes differentially expressed between Xist-induced (+dox) and uninduced (control) in *Pcgf3*$^{fl/fl}$*Pcgf5*$^{-/-}$ (left) and *Pcgf3*$^{-/-}$*Pcgf5*$^{-/-}$ (right) mESCs on Xist transgene bearing chromosome 16. Genes with false discovery rate (FDR) < 0.05 are depicted in violet; FDR > 0.05 and <0.1 are in green. (**F**) Heatmap showing expression change between Xist-induced (+dox) and uninduced (control) mESCs for all genes significantly misregulated on chromosome 16 in *Pcgf3*$^{fl/fl}$*Pcgf5*$^{-/-}$ (FDR < 0.1), together with expression changes for the same genes in *Pcgf3*$^{-/-}$*Pcgf5*$^{-/-}$ mESCs.

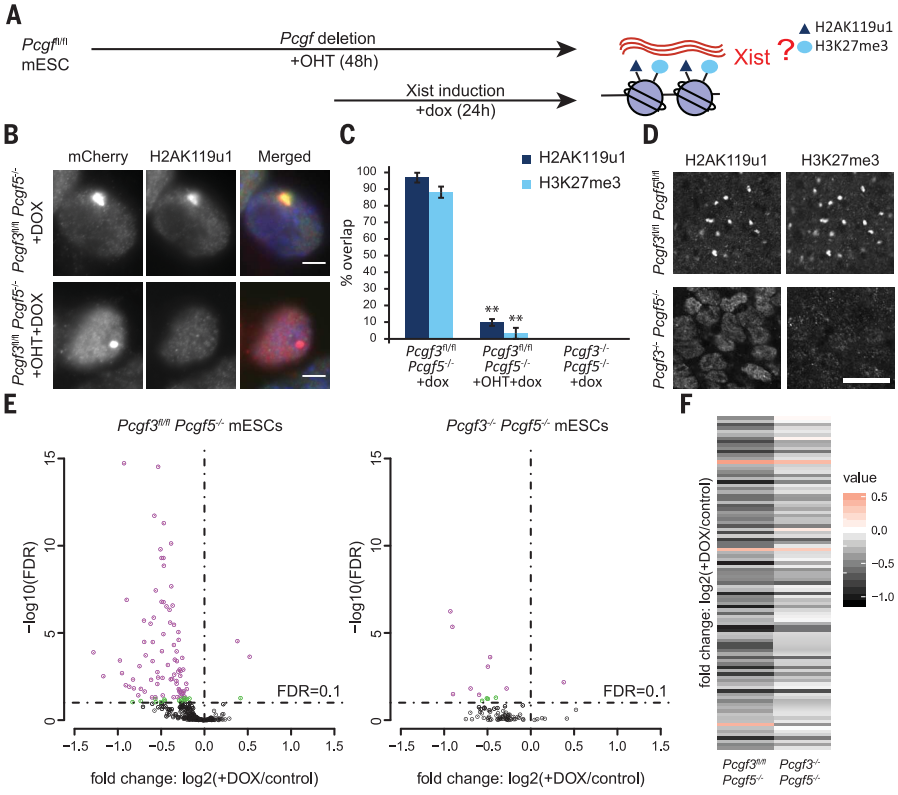

which the embryos and placentas appeared grossly normal. However, in female *Pcgf3*$^{-/-}$*Pcgf5*$^{-/-}$ conceptuses, the embryo was extensively degraded (supplementary text S12 and fig. S12A). Histological analysis revealed some defects in placentas from male embryos, but more strikingly, female placentas lack trophoblasts altogether and as a consequence fail to form a labyrinth (supplementary text S12 and fig. S12B). Other genotypes, including *Pcgf3* and *Pcgf5* single homozygous embryos, were found at approximately the expected Mendelian ratio (fig. S12C).

Female-specific phenotypes in *Pcgf3*$^{-/-}$*Pcgf5*$^{-/-}$ embryos suggest that Xist-mediated silencing may be compromised. To test this directly, we performed RNA-sequencing (RNA-seq) analysis, comparing silencing in the presence or absence of Xist-dependent Polycomb recruitment in mESCs (*Pcgf3*$^{fl/fl}$*Pcgf5*$^{-/-}$ compared with *Pcgf3*$^{-/-}$*Pcgf5*$^{-/-}$) (supplementary text S13). The results demonstrate strong abrogation of Xist-mediated gene silencing, affecting genes across the entire chromosome (Fig. 4, E and F, and fig. S13, A to C). We conclude that loss of both PRC1 and PRC2 substantially compromises Xist-mediated silencing.

This study redefines the molecular pathway for Polycomb recruitment by Xist RNA, as summarized in fig. S14. Our findings further provide proof of principle that noncanonical PRC1 and associated H2AK119u1 can function to initiate the formation of Polycomb domains in a physiological context. In future studies, it will be important to understand how PCGF3/5–PRC1 interacts with the Xist XN region and to determine whether the same pathway is used by other long noncoding RNAs.

REFERENCES AND NOTES

1. Y. B. Schwartz, V. Pirrotta, *Nat. Rev. Genet.* **14**, 853–864 (2013).
2. M. de Napoles *et al.*, *Dev. Cell* **7**, 663–676 (2004).
3. J. Silva *et al.*, *Dev. Cell* **4**, 481–495 (2003).
4. K. Plath *et al.*, *Science* **300**, 131–135 (2003).
5. J. Zhao, B. K. Sun, J. A. Erwin, J. J. Song, J. T. Lee, *Science* **322**, 750–756 (2008).
6. A. Cerase *et al.*, *Proc. Natl. Acad. Sci. U.S.A.* **111**, 2235–2240 (2014).
7. S. T. da Rocha *et al.*, *Mol. Cell* **53**, 301–316 (2014).
8. S. Schoeftner *et al.*, *EMBO J.* **25**, 3110–3122 (2006).
9. L. Tavares *et al.*, *Cell* **148**, 664–678 (2012).
10. C. Chu *et al.*, *Cell* **161**, 404–416 (2015).
11. N. P. Blackledge *et al.*, *Cell* **157**, 1445–1459 (2014).
12. S. Cooper *et al.*, *Cell Reports* **7**, 1456–1470 (2014).
13. R. Kalb *et al.*, *Nat. Struct. Mol. Biol.* **21**, 569–571 (2014).
14. S. Cooper *et al.*, *Nat. Commun.* **7**, 13661 (2016).
15. Materials and methods are available as supplementary materials.
16. Y. A. Tang *et al.*, *Epigenet. Chromatin* **3**, 10 (2010).
17. Z. Gao *et al.*, *Mol. Cell* **45**, 344–356 (2012).
18. B. Moindrot *et al.*, *Cell Reports* **12**, 562–572 (2015).
19. E. García, C. Marcos-Gutiérrez, M. del Mar Lorente, J. C. Moreno, M. Vidal, *EMBO J.* **18**, 3404–3418 (1999).
20. R. Arrigoni *et al.*, *FEBS Lett.* **580**, 6233–6241 (2006).

ACKNOWLEDGMENTS

We thank the Brockdorff and Koseki laboratories for comments, A. Otte and F. Barr for antibodies, R. Klose for plasmids and antibodies, A. Bassett for facilitating CRISPR/Cas9 mutagenesis, D. Moralli and C. Green for transgene mapping, and E. Hookway for sequencing. Work in the N.B. laboratory was funded by grants from the Wellcome Trust (103768 and 091911) and European Research Council (340081). M.A. was funded by a Ph.D. fellowship from Fundação para a Ciência e Tecnologia, Portugal (SFRH/BD/51706/2011). H.K. was funded by Core Research for Evolutional Science and Technology from the Japan Science and Technology Agency–Agency for Medical Research and Development. A.M. was funded by Wellcome Trust (102811). Accession no. ArrayExpress E-MTAB-5642. D.B. was funded by a Wellcome Trust Ph.D. studentship (092926).

SUPPLEMENTARY MATERIALS

www.sciencemag.org/content/356/6342/1081/suppl/DC1
Materials and Methods
Supplementary Text
Figs. S1 to S14
References (*21*–*34*)
Table S1
Movies S1 to S6

20 October 2016; accepted 12 May 2017
10.1126/science.aal2512

PCGF3/5–PRC1 initiates Polycomb recruitment in X chromosome inactivation

Mafalda Almeida, Greta Pintacuda, Osamu Masui, Yoko Koseki, Michal Gdula, Andrea Cerase, David Brown, Arne Mould, Cassandravictoria Innocent, Manabu Nakayama, Lothar Schermelleh, Tatyana B. Nesterova, Haruhiko Koseki and Neil Brockdorff

Science **356** (6342), 1081-1084.
DOI: 10.1126/science.aal2512

Polycomb steps to inactivate X

XX females silence one of their X chromosomes. This involves a process whereby a noncoding RNA known as Xist coats one of the X chromosomes and recruits chromatin silencing factors. The Polycomb complexes PRC1 and PRC2 are also known to be involved in X chromosome inactivation. Almeida *et al.* elucidate a key role of a specific complex, PCGF3/5-PRC1, in initiating Polycomb recruitment by Xist RNA. They further demonstrate that Polycomb recruitment is critical for Xist-mediated chromosome silencing and female embryogenesis.

Science, this issue p. 1081